Cancer Letters 447 (2019) 141–153

Contents lists available at ScienceDirect

Cancer Letters

journal homepage: www.elsevier.com/locate/canlet

Original Articles

C-terminal HSP90 inhibitor L80 elicits anti-metastatic effects in triple-negative breast cancer via STAT3 inhibition

Tae-Min Cho[a,b,1], Ji Young Kim[a,1], Yoon-Jae Kim[a,c], Daeil Sung[a,b], Eunhye Oh[a,b], Seojin Jang[a,b], Lee Farrand[d], Van-Hai Hoang[e], Cong-Truong Nguyen[e], Jihyae Ann[e], Jeewoo Lee[e,**], Jae Hong Seo[a,b,*]

[a] Division of Medical Oncology, Department of Internal Medicine, Korea University College of Medicine, Korea University, Seoul, 152-703, Republic of Korea
[b] Brain Korea 21 Program for Biomedical Science, Korea University College of Medicine, Korea University, Seoul, 152-703, Republic of Korea
[c] Department of Biomedical Research Center, Korea University Guro Hospital, Korea University, Seoul, 08308, Republic of Korea
[d] AusHealth Research, 65 Hardys Rd, Underdale, Adelaide, South Australia, 5032, Australia
[e] Laboratory of Medicinal Chemistry, College of Pharmacy, Seoul National University, Seoul, 08826, Republic of Korea

ARTICLE INFO

Keywords:
C-terminal HSP90 inhibitor
L80
Triple-negative breast cancer
Cancer stem cells
STAT3
Metastasis

ABSTRACT

Triple-negative breast cancer (TNBC) is an aggressive heterogeneous disease with a divergent profile. It has an earlier tendency to form metastases and is associated with poor clinical outcomes due to the limited treatment options available. Heat-shock protein (HSP90) represents a potential treatment target as it promotes tumor progression and metastasis by modulating the maturation and stabilization of signal transduction proteins. We sought to investigate the efficacy of the C-terminal HSP90 inhibitor L80 on cell proliferation, breast cancer stem cell (BCSC)-like properties, tumor growth and metastasis. L80 suppressed cell viability and concomitantly inhibited AKT/MEK/ERK/JAK2/STAT3 signaling in TNBC cells but did not induce cytotoxicity in normal cells. L80 effectively targeted BCSC-like traits, together with significant reductions in the CD44high/CD24low-population, ALDH1 activity and mammosphere forming-ability. In support of the *in vitro* observations, L80 administration caused significant impairment in tumor growth, angiogenesis and distant metastases in an orthotopic allograft model with BCSC-enriched cells *in vivo*. These phenomena were associated with the suppression of BCSC-like characteristics and STAT3 dysfunction. Our findings highlight properties of the L80 compound that may be useful in suppressing metastatic TNBC.

1. Introduction

Triple-negative breast cancer (TNBC) accounts for 10–15% of all diagnosed breast cancers and has an aggressive clinical course due to a lack of therapeutic cellular targets [1]. Accumulating clinical evidence demonstrates that TNBC is biologically more aggressive and has a higher Ki-67 proliferation index with greater metastatic potential than other breast cancer subtypes [2,3]. Consensus toward a standard therapeutic strategy is lacking, and the overall five-year survival rate is less than 30% in TNBC patients who present with a distant recurrence [4].

Heat-shock protein 90 (HSP90) is a ubiquitous molecular chaperone that is evolutionally conserved and highly abundant, comprising 1–2% of total cellular protein under normal physiological conditions [5]. During cancer progression, this proportion increases by 2–10-fold in tumor cells [6]. HSP90 plays important roles in numerous biological functions and diverse processes including cell survival, proliferation, cancer progression and metastasis by regulating stability, maturation and the conformational changes of various proteins [7–9]. Elevated HSP90 levels are frequently observed in TNBC patients, which is associated with a higher risk of recurrence, distant metastasis and a poor prognosis [10]. HSP90 dysfunction with natural and synthetic inhibitors attenuates cell proliferation, survival and cell dissemination in many cancer types via dysregulation of HSP90 client oncoproteins including HER2, EGFR, VEGF, JAK, STAT, and AKT [11–14].

Of particular note, HSP90 is essential for the functional competence of STAT3 activity that governs the tumor microenvironment and cancer

* Corresponding author. Korea University, Guro Hospital Campus, 97 Gurodong-gil, Guro-gu, Seoul, 08308, Republic of Korea. Tel.: +82 2 2626 3059; fax: +82 2 862 6453.
** Corresponding author. Tel.: +82 2 880 7846; fax: +82 2 888 0649.
E-mail addresses: jeewoo@snu.ac.kr (J. Lee), cancer@korea.ac.kr (J.H. Seo).
[1] T-M. Cho and JY. Kim contributed equally to this work.

https://doi.org/10.1016/j.canlet.2019.01.029
Received 25 October 2018; Received in revised form 28 December 2018; Accepted 22 January 2019

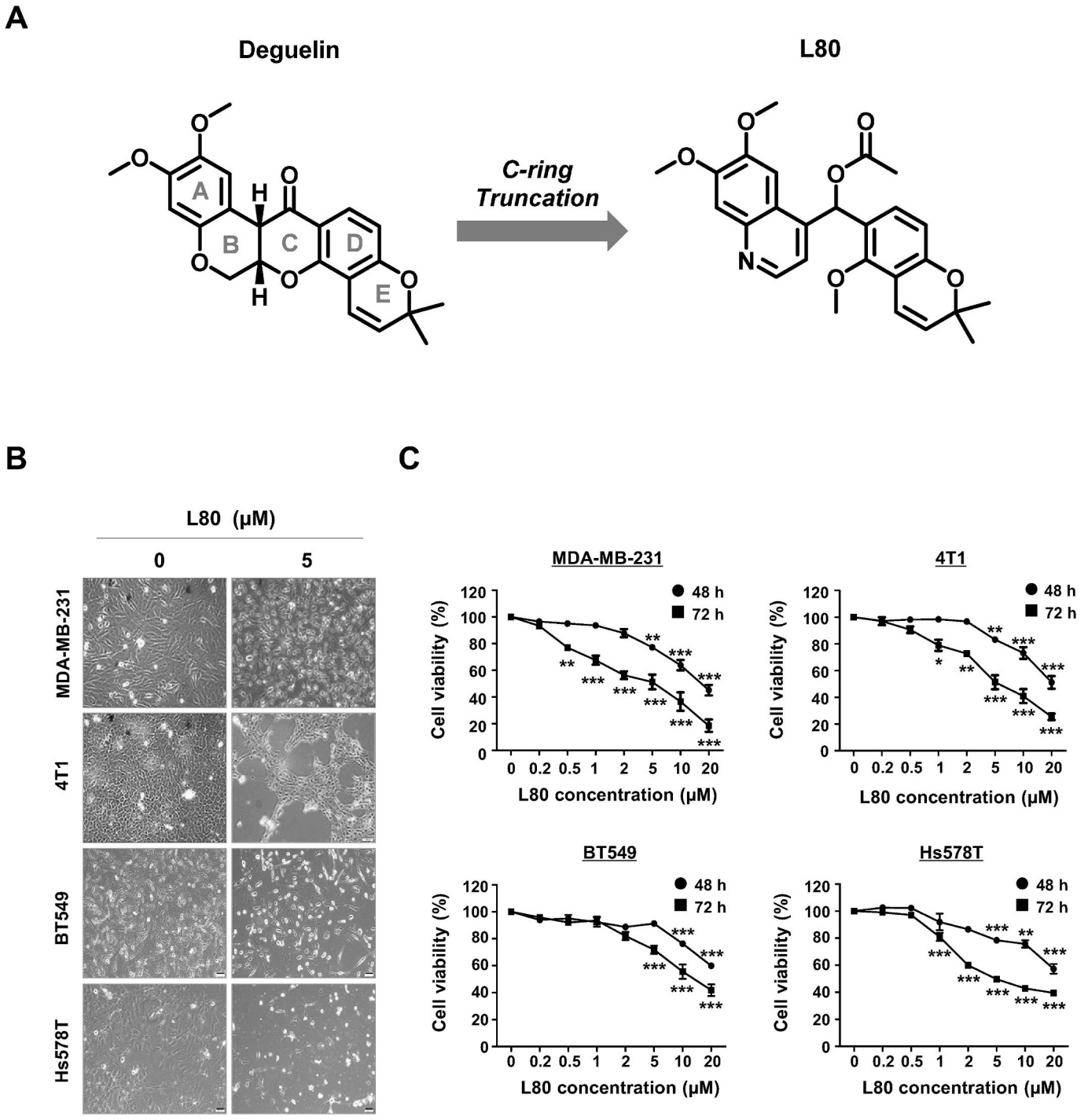

Fig. 1. L80 suppresses TNBC cell viability in a dose- and time-dependent manner. (A) Chemical structures of deguelin and L80. (B) Changes in cellular morphology in MDA-MB-231, 4T1, BT549 and Hs578T cells after L80 (5 μM) treatment for 72 h as seen through phase contrast microscopy. (C) Effect of L80 on cell viability. Cells were treated with various concentrations of L80 (0.2–20 μM) for 48 h and 72 h. Cell viability was determined by MTS assay (*$p < 0.05$, versus DMSO control). The results are presented as mean ± SEM of at least three independent experiments and analyzed by two-way ANOVA followed by Bonferroni's *post hoc* test.

progression [15]. The constitutive activation of STAT3 in TNBC is associated with drug resistance to chemotherapy and a shorter survival period [16,17]. Blockage of the JAK/STAT axis elicits anti-angiogenic and -metastatic effects via suppression of the downstream signaling pathways involved [18–20]. A specific and direct interaction between HSP90 and STAT3 has been observed, which is a prerequisite for STAT3 interaction with JAK kinases, phosphorylation, dimerization, and nuclear translocation of STAT3, contributing to tumor cell survival [15,21]. Therefore, HSP90 inhibition might serve to simultaneously block both HSP90 function and STAT3 signaling.

HSP90 consists of three distinct domains, an N-terminal ATP-binding domain, a middle domain, and a C-terminal dimerization domain [9]. To date, the majority of HSP90 inhibitors in drug development target the N-terminal ATP-binding domain. Although several N-terminal HSP90 inhibitors are in clinical trials, none are currently available for routine cancer treatment [11,22]. The major impediment for N-terminal inhibitors is the induction of the heat shock response (HSR) and considerable upregulation of co-chaperones (HSP70 and

HSP27) leading to the suppression of apoptosis via interference with key apoptotic-factors such as caspases, death receptors, bax and formation of the apoptosome [23,24]. In this context, further prospects in drug discovery of HSP90 inhibitors will need to focus on targeting the interaction of HSP90 with co-chaperone proteins (CDC37, HSP70 and HSF-1), including the C-terminal dimerization domain or downstream clients [22].

We synthesized the C-ring truncated deguelin derivative L80 as a C-

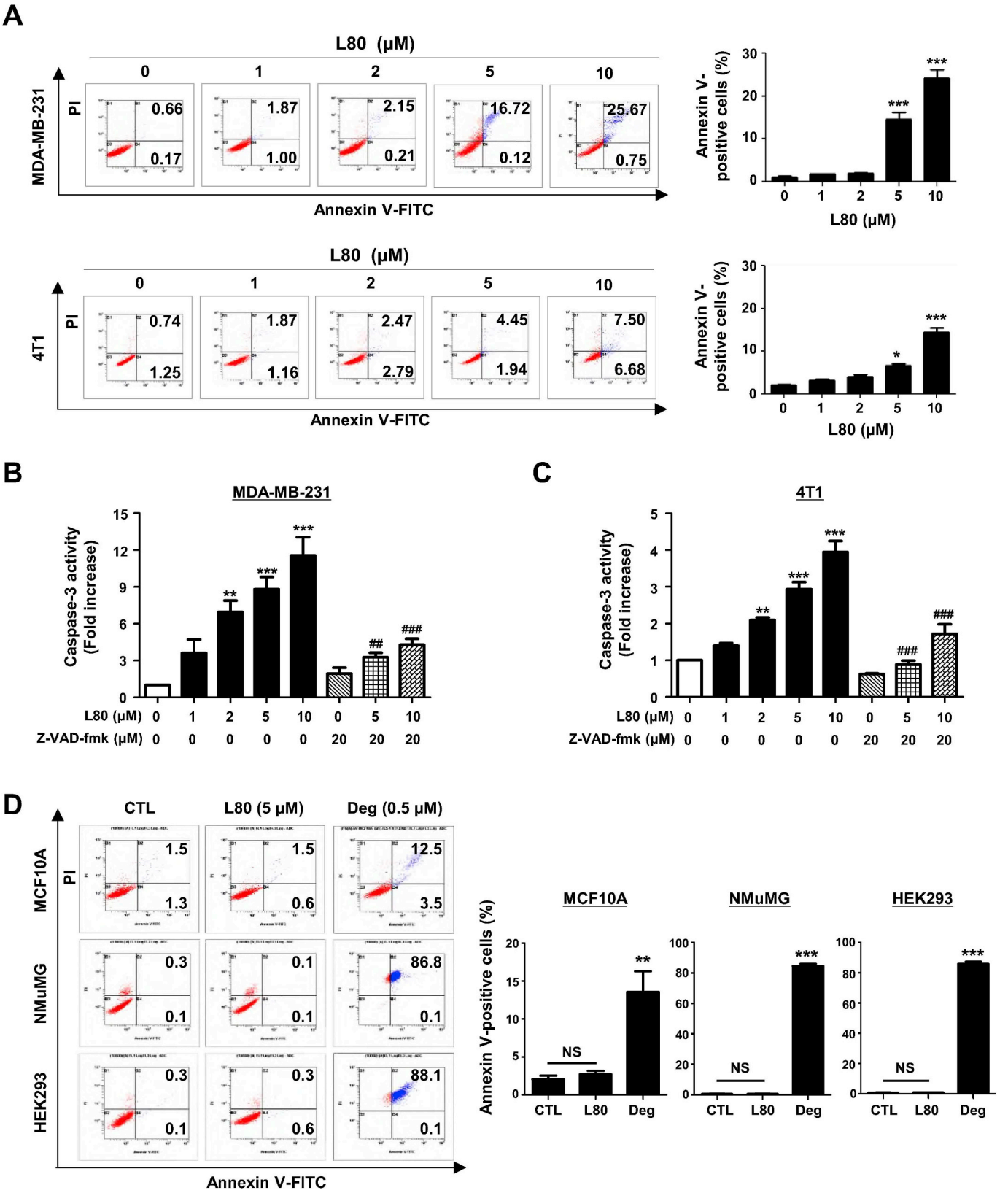

(caption on next page)

Fig. 2. L80-induces apoptosis accompanied by caspase-3 activity. (A) MDA-MB-231 and 4T1 cells were treated with L80 (0–10 μM, 72 h) and early and late apoptosis assays with annexin V/PI staining were performed with flow cytometry. The percentages of the annexin V-positive cell populations have been quantified (right panel, $*p < 0.05$). (B–C) Effect of L80 on caspase-3 activity. Cells were pre-cultured with Z-VAD-fmk (20 μM, 1 h) before L80 treatment (0–10 μM, 72 h) and caspase-3 activity was analyzed by spectrophotometer. Data were analyzed by one-way ANOVA followed by Bonferroni's *post hoc* test, ($**p < 0.01$, DMSO vs L80; $\#\#p < 0.01$, L80 treatment alone vs combination treatment with Z-VAD-fmk and L80). (D) L80 does not affect apoptosis in normal cells *in vitro*. Normal human mammary epithelial MCF10A, normal murine mammary gland NMuMG cells or normal human embryonic kidney HEK293 cells were treated with L80 (5 μM) or deguelin (0.5 μM) for 72 h. Apoptosis assays with annexin V/PI staining were performed using flow cytometry, and the percentages of the annexin V-positive cells were quantified. The results are presented as mean ± SEM of at least three independent experiments. Data were analyzed by Student's t-test ($**p < 0.01$, DMSO vs deguelin (Deg); NS, not significant, DMSO vs L80).

terminal HSP90 inhibitor and demonstrated that it possesses strong anti-tumor activity in non-small cell lung cancer (NSCLC) via HIF-1α degradation mediated by the ubiquitin-proteasome pathway [25]. In the present study, we sought to investigate the mechanism of action of L80 responsible for its novel effects against cell proliferation and BCSC properties *in vitro*, as well as angiogenesis, tumor growth and metastasis *in vivo*.

2. Materials and methods

2.1. Reagents and antibodies

A detailed description of the synthesis of L80 is described in our previous report [25]. Z-VAD-fmk, Triton X-100, propidium iodide (PI), corn oil and dimethyl sulfoxide (DMSO) were obtained from Sigma-Aldrich (St. Louis, MO). Phosphatase inhibitor and protease inhibitor cocktail tablets were purchased from Roche Applied Sciences (Penzberg, GER). The antibodies that were used include: STAT3, Ki-67, CD31, ALDH1A1 (Abcam, MA); anti-AKT, phospho-AKT (Ser473), ERK, phospho-ERK (Thr202/Tyr204), JAK2, phospho-JAK2 (Tyr1007/1008), phospho-STAT3 (Tyr705), CD49f, vimentin, Nanog, Oct4 (Cell Signaling, CA); survivin, MEK, phospho-MEK (Ser218/222), HSP70, cyclin D1 (Santa Cruz Biotechnology, Santa Cruz,CA); β-actin (Sigma-Aldrich, Saint Louis, MO). The secondary antibodies were horseradish peroxidase (HRP)-conjugated anti-rabbit and mouse IgG (Bio-Rad Laboratories, CA); and Alexa Fluor-594 goat anti-mouse IgG (Invitrogen, CA).

2.2. Breast cancer cell culture

The TNBC cell lines MDA-MB-231 (PerkinElmer, Inc. CT), Hs578T (American Type Culture Collection, ATCC), BT-549 and 4T1-Luc (Japanese Collection of Research Bioresources Cell Bank, JCRB), and the normal murine mammary gland epithelial cell line NMuMG (American Type Culture Collection) and the normal human embryonic kidney cell line HEK293 (JCRB) were cultured in MEM or RPMI 1640 (Gibco, MD) containing 10% fetal bovine serum (FBS), streptomycin-penicillin (100 U/ml) and Fungizone (0.625 μg/mL). Normal human mammary epithelial MCF10A (ATCC) cells were cultured in Mammary Epithelial Cell Growth Medium (MEGM), including hEGF, insulin, hydrocortisone and bovine pituitary extract (SingleQuots™ Kit, Lonza, CA) containing streptomycin-penicillin (100 U/ml). Cells were incubated at 37 °C in an atmosphere of 5% CO_2.

2.3. Cell viability assay

Cell viability was measured using the CellTiter 96* Aqueous One Solution Cell Proliferation Assay [MTS, 3-(4,5-dimethylthiazol-2-yl)-5-(3-carboxymethoxyphenyl)-2-(4-sulfophenyl)-2H-tetrazolium] (Promega, WI), as previously described [26].

2.4. Annexin V/PI assay

Cells were stained using a FITC-conjugated Annexin V apoptosis detection kit (BD Biosciences, Franklin Lakes, NJ) according to the manufacturer's protocol. Stained cells were analyzed by flow cytometry using a Beckman Coulter Expo (Brea, CA).

2.5. Caspase-3 activity assay

Caspase-3 activity was measured using caspase 3 colorimetric assay kits, according to the manufacturer's instructions (Sigma-Aldrich, MO). Caspase-3 activity was analyzed by absorbance at 405 nm with a Spectramax Plus384 microplate analyzer (Molecular Devices, CA).

2.6. $CD44^{high}/CD24^{low}$ staining

$CD44^{high}/CD24^{low}$ staining was used to identify BCSC-like cells. Cells were incubated for 30 min at 4 °C with FITC- and PE-conjugated anti-mouse IgG or FITC-conjugated anti-CD24 and PE-conjugated anti-CD44 antibodies (BD Biosciences) and analyzed by flow cytometry.

2.7. Aldefluor-positivity assay

An Aldefluor assay kit (Stemcell Technologies, Vancouver, BC) was used to assess ALDH1 activity, as previously described [27]. As a specific inhibitor of ALDH1, 50 mM diethylamino-benzaldehyde (DEAB) was used to define the Aldefluor-positive population with a flow cytometer.

2.8. Western blot analysis

The procedures were performed as previously described [26]. Primary antibody dilutions were: [AKT (1:2000), phospho-AKT (1:2000), ERK (1:2000), phospho-ERK (1:2000), JAK2 (1:2000), phospho-JAK2 (1:2000) (Tyr1007/1008), STAT3 (1:3000), phospho-STAT3 (1:2000), cyclin D1 (1:3000), survivin (1:2000), MEK (1:3000), phospho-MEK (1:3000), HSP70 (1:3000), Nanog (1:2000), Oct4 (1:2000) or β-actin (1:5000)] and membranes were incubated with HRP-conjugated rabbit or mouse secondary antibody (1:3000–1:10,000). Signal intensity was detected using a Chemiluminescence Kit (Thermo Fisher Scientific Fremont, CA) on X-ray film (Agfa Healthcare, Mortsel, Belgium) and quantitated using AlphaEaseFC software (Alpha Innotech, San Leandro, CA).

2.9. Allograft in vivo experiments and bioluminescence imaging

All animal procedures were carried out in accordance with animal care guidelines approved by the Korea University Institutional Animal Care and Use Committee (IACUC). Five-week-old female BALB/c mice were obtained from the Shizuoka Laboratory Animal Center (Shizuoka, Japan) and housed in a specific pathogen-free environment. The animals were acclimated for 1 week prior to the study and had free access to food and water. 1×10^5 cells from 4T1 mammospheres were implanted subcutaneously in the right flank of 6-week-old BALB/c female mice (n = 8/each group). After 1 week, vehicle (DMSO/corn oil, 1:9) or L80 (20 mg/kg/day, every other day) was administered intraperitoneally for 27 days, and tumor volumes were measured using a caliper and calculated using formula $V = (\text{Length} \times \text{Width}^2)/2$. The animals were then anesthetized and subjected to NightOWL LB983 bioluminescence imaging (BLI) (Berthold Technologies, TN). The procedures were performed as previously described [28].

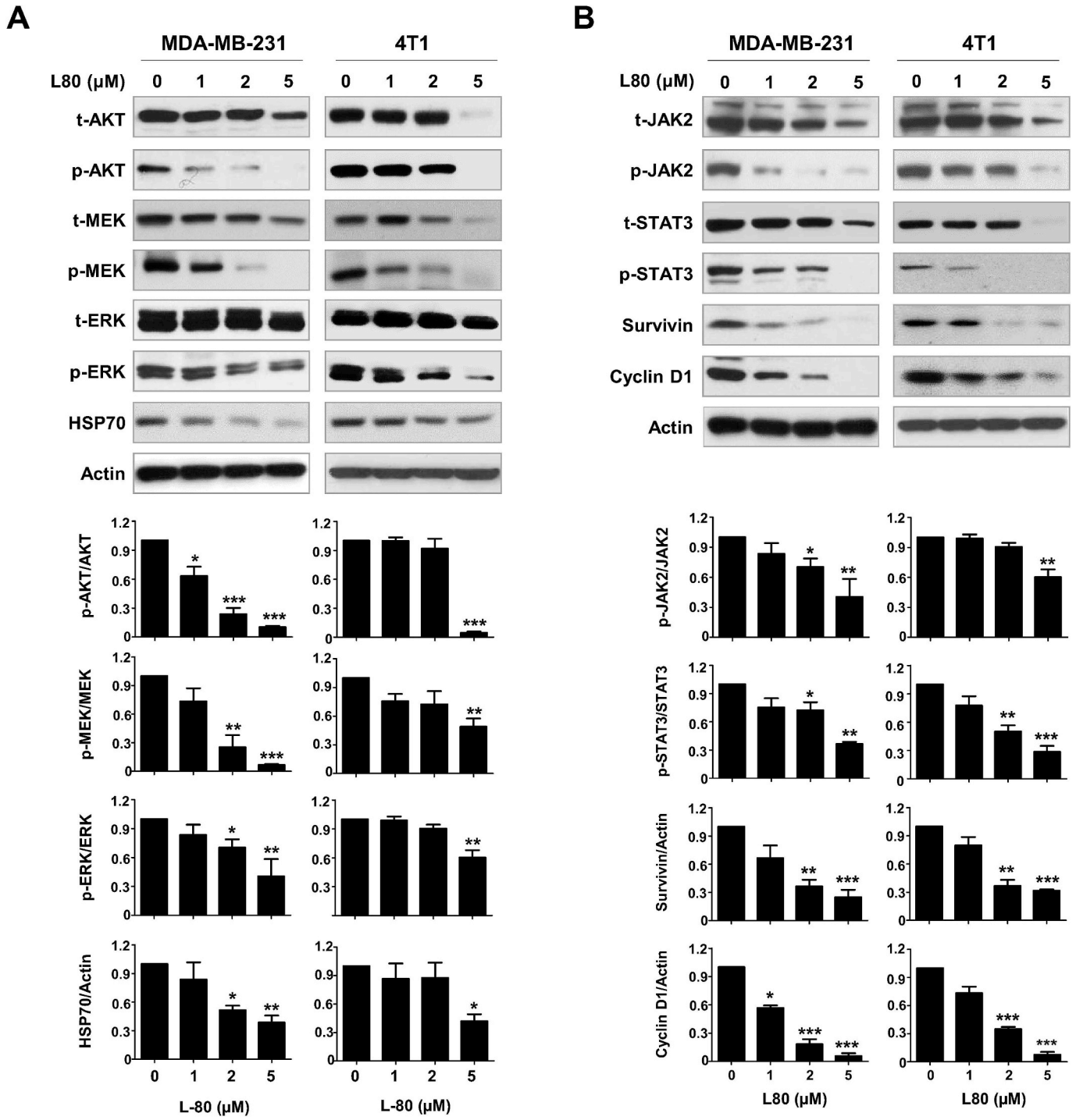

Fig. 3. Effect of L80 treatment on HSP90 client proteins in TNBC cells. (A) Immunoblot analyses of AKT, phospho-AKT (Ser473), MEK, phospho-MEK (Ser218/222), ERK, phospho-ERK (Thr202/Tyr204) and HSP70 protein expression in MDA-MB-231 and 4T1 cells following exposure to L80 (1–5 μM, 72 h). Actin was used as a loading control. Quantitative graphs represent the ratio of phosphorylated-/total-proteins, and the ratio of HSP70/actin in the presence or absence of L80 (bottom panel, $*p < 0.05$). (B) Effect of L80 (1–5 μM, 72 h) on expression of STAT3 signaling-related factors in TNBC cells *in vitro*. Quantitative graphs represent the ratio of phosphorylated-/total-proteins, and the ratio of survivin/actin and cyclin D1/actin in the presence or absence of L80 (bottom panel, $*p < 0.05$). The results are presented as mean ± SEM of at least three independent experiments analyzed by one-way ANOVA followed by Bonferroni's *post hoc* test.

2.10. Immunohistochemistry and in-situ localization of apoptosis (TUNEL)

Immunohistochemistry analysis was performed as previously described [29]. Tissue sections with primary antibodies (Ki-67; 1:150, CD49f; 1:150, ALDH1A1; 1:150, CD31; 1:100 or vimentin; 1:150) in antibody-diluent (Dako, Glostrup, Denmark) were incubated overnight at 4 °C. For secondary antibody reactions, the sections were incubated with fluorescence-conjugated secondary antibody at RT for 2 h, followed by ProLong gold antifade reagent with DAPI (Life Technologies, CA). Phospho-JAK2 (1:100) and phospho-STAT3 (1:100) staining was performed using a Vectastain ABC kit (Vector Laboratories, CA) with diaminobenzidine (DAB, GBI labs, WA) followed by hematoxylin counterstaining (Sigma, MO) in accordance with the manufacturer's instructions. In situ TUNEL was carried out on tissue sections using a

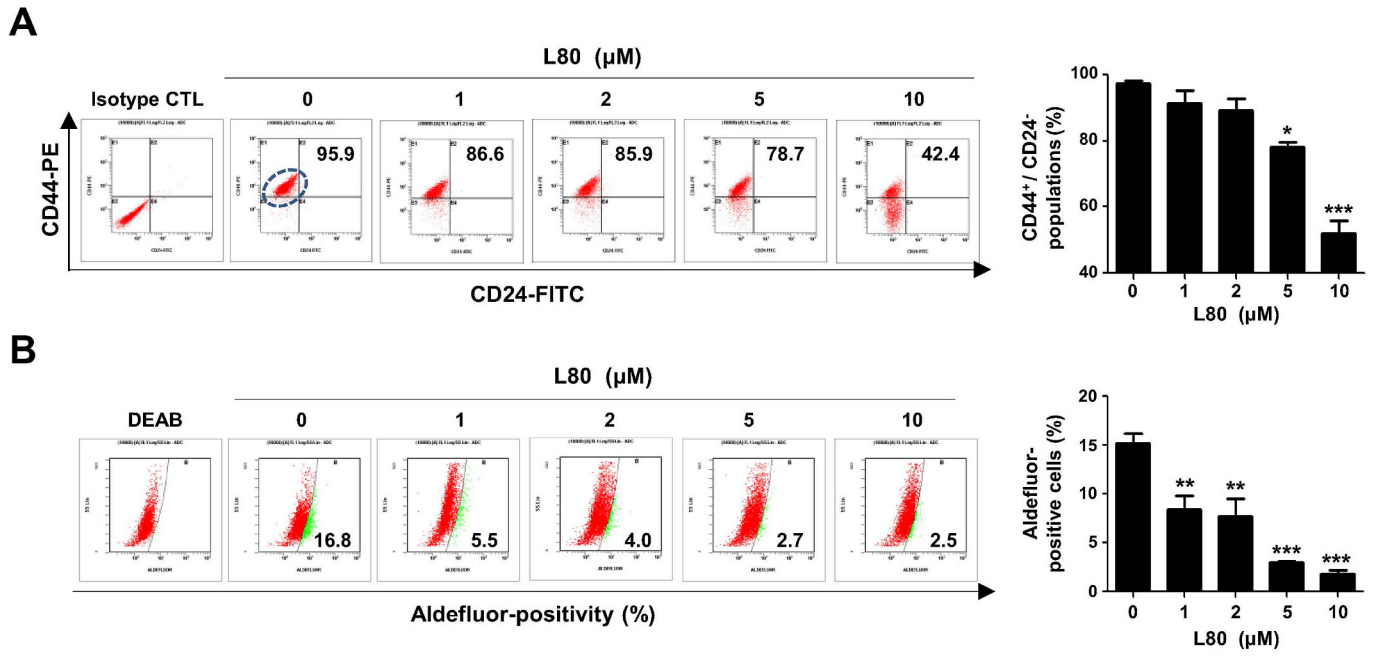

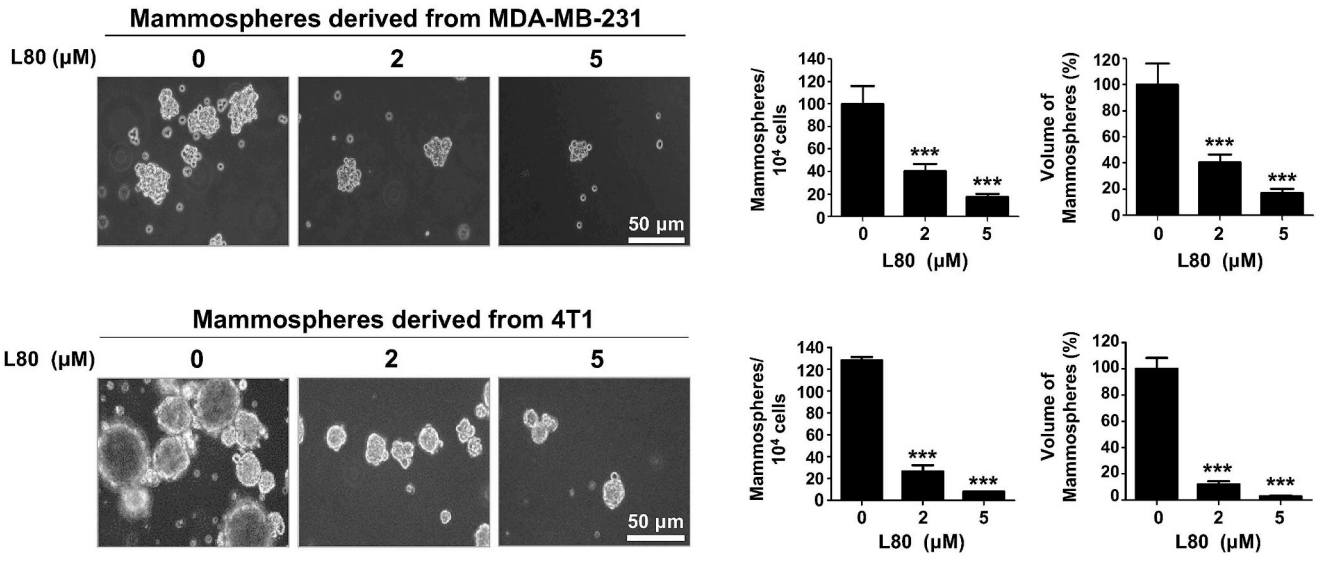

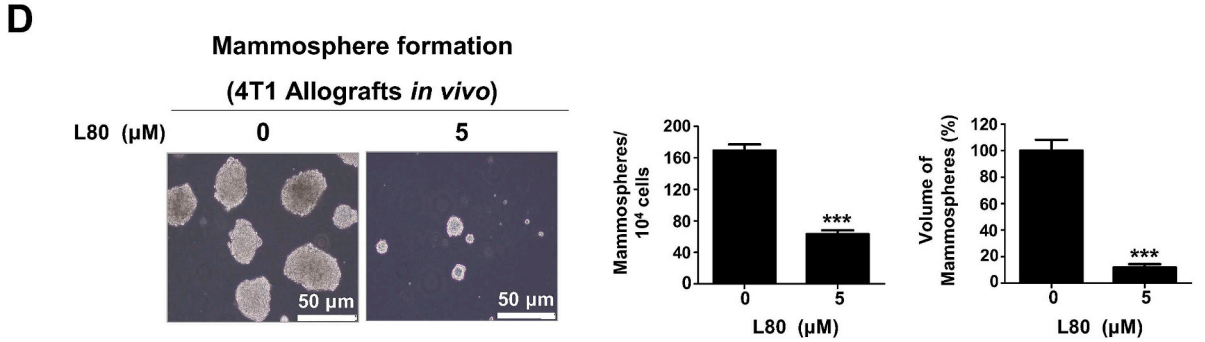

(caption on next page)

Fig. 4. L80 suppresses BCSC-like properties. (A–B) After exposure to L80 (1–10 μM, 72 h), $CD44^{high}/CD24^{low}$ populations and ALDH1 activity in MDA-MB-231 cells were evaluated by flow cytometry. The quantitative graph represents the percentage of $CD44^{high}/CD24^{low}$ populations (A, $*p < 0.05$) and Aldefluor-positive cells (B, $**p < 0.01$) are shown in the right panels, respectively. (C) MDA-MB-231 (1×10^5 cells/ml) and 4T1 (5×10^4 cells/ml) were cultured in serum-free suspension conditions in ultralow attachment plates in the presence or absence of L80 (2 and 5 μM) for 4 days. The number and volume of mammospheres was quantified by optical microscopy (right panels, $***p < 0.001$). (D) Effect of L80 on mammosphere formation in an allograft model with 4T1 cells *in vivo*. Dissociated single cells (1×10^5/ml) from allograft tumors (300–350 mm^3) were plated in ultralow attachment dishes and cultured in the presence or absence of L80 (5 μM) for 4 days. The number and volume of mammospheres was quantified (right panels, $***p < 0.001$). Data were analyzed by Student's t-test or one-way ANOVA followed by Bonferroni's *post hoc* test.

TUNEL kit (Roche Applied Sciences, Penzberg, GER) in accordance with the manufacturer's instructions.

2.11. Mammosphere formation in vitro and in vivo assay

In vitro and *in vivo* mammosphere-forming assays were performed as previously described [28]. In brief, cells were plated in ultralow attachment dishes and cultured in HuMEC basal serum free medium (Gibco, MD), supplemented with B27 (1:50, Invitrogen), 20 ng/mL basic fibroblast growth factor (bFGF, Sigma), 20 ng/mL human epidermal growth factor (EGF, Sigma), 4 μg/ml heparin, 1% antibiotic-antimycotic, and 15 μg/mL gentamycin at 37 °C in an atmosphere of 5% CO2. The number and volume of the mammospheres were determined under an Olympus IX 71 inverted microscope.

2.12. MMP-2 and MMP-9 ELISA assay

The matrix metalloproteinase MMP-2 and MMP-9 levels in mouse serum were measured using ELISA kits (R&D systems, Minneapolis, MN), according to the manufacturer's instructions. The quantity of MMP-2 and MMP-9 was determined by measuring the absorbance at 450 nm with a Spectramax MAX 190 microplate reader (Molecular Devices, CA).

2.13. Statistical analysis

All data were analyzed using GraphPad Prism 5.0 statistical software (San Diego, CA). The results are presented as mean ± SEM of at least three independent experiments. Data were analyzed by student's *t*-test, and one- or two-way ANOVA as appropriate. Significance between multiple experimental groups was determined using the Bonferroni *post hoc* test and defined at $p^* < 0.05$.

3. Results

3.1. L80 exerts cytotoxic effects on TNBC cells in vitro

We have previously synthesized the C-ring truncated deguelin derivative L80 [25], (Fig. 1A). We first sought to examine the cytotoxic effect of L80 on cell viability and apoptosis in MDA-MB-231, 4T1, BT549 and Hs578T cells *in vitro*. Following exposure to L80 (5 μM) for 72 h, TNBC cells exhibited significant morphological changes with concomitant cytoplasmic shrinkage and cellular rounding (Fig. 1B). MTS assays revealed that L80 (0.2–20 μM, 48–72 h) significantly suppressed cell viability in TNBC cells in a dose- and time-dependent manner ($p < 0.05$, Fig. 1C).

3.2. L80 induces apoptosis in a caspase-dependent manner

L80-induced apoptosis was evaluated by annexin V assay. A significant increase in early and late apoptotic cells in the presence of L80 (5–10 μM) was observed ($p < 0.05$, Fig. 2A). This effect was accompanied by caspase-3 activation. The pretreatment with the pan-caspase inhibitor Z-VAD-fmk (20 μM, 1 h) significantly attenuated L80-induced caspase-3 activity (Fig. 2B and C).

We additionally examined the effects of L80 and its parent drug deguelin on apoptosis in normal human mammary epithelial MCF10A, normal murine mammary gland NMuMG and normal human embryonic kidney HEK293 cells. Annexin-V/PI staining analysis revealed that there were no statistically significant differences between CTL and L80 treatment (5 μM, 72 h) in MCF10A, NMuMG and HEK293 cells, indicating that L80 exhibits minimal cytotoxicity in normal cells (NS; not significant). Deguelin (0.5 μM, 72 h) elicited a significant effect on apoptosis in normal cells, which was observed at a 10-fold lower concentration ($p < 0.01$, Fig. 2D).

3.3. L80 inhibits phosphorylation of AKT, MEK/ERK and JAK2/STAT3 signaling

AKT, MEK, JAK2, and STAT3 are the major client proteins of HSP90, and their function and activation are ultimately governed by HSP90 action [7,15,21]. We observed that L80 treatment not only downregulated AKT, MEK, and ERK protein content, but also markedly reduced their phosphorylation. Quantitative data further showed a significant reduction in the activation of these HSP90 client kinases and HSP70 expression in the presence of L80 ($p < 0.05$, http://journals.plos.org/plosone/article?id=10.1371/journal.pone.0049194 Fig. 3A). Of particular note, STAT3 is constitutively activated in all breast cancer sub-types but it is most often associated with TNBC and its cytosolic and nuclear activations are mediated by HSP90 activity [21,30,31]. Exposure to L80 treatment was found to downregulate phospho-JAK2 and phospho-STAT3 (Tyr705) in MDA-MB-231 and 4T1 cells ($p < 0.05$, http://journals.plos.org/plosone/article?id=10.1371/journal.pone.0049194 Fig. 3B). This phenomenon was accompanied by downregulation of STAT3 downstream factors including survivin and cyclin D1, as evidenced by significant reductions in their mRNA abundance ($p < 0.01$, Supplementary Fig. S1) and protein content ($p < 0.05$, http://journals.plos.org/plosone/article?id=10.1371/journal.pone.0049194 Fig. 3B) *in vitro*.

3.4. L80 targets BCSC-like properties in TNBC cells

A significant relationship between constitutive activation of STAT3 and BCSC-like features was observed [28,30,32,33]. Since L80 significantly inhibits STAT3 activation, we next examined whether L80 regulates BCSC-like properties and assessed the stem cell surface markers $CD44^{high}/CD24^{low}$ and the progenitor marker aldehyde dehydrogenase 1 (ALDH1), as well as *in vitro* mammosphere-forming ability. Significant reductions in $CD44^{high}/CD24^{low}$ stem-like populations ($p < 0.05$, http://journals.plos.org/plosone/article?id=10.1371/journal.pone.0049194 Fig. 4A) and ALDH1 activity ($p < 0.01$, http://journals.plos.org/plosone/article?id=10.1371/journal.pone.0049194 Fig. 4B) were observed in MDA-MB-231 cells following L80 treatment. Mammospheres are known to be highly enriched with putative cancer stem cells harboring self-renewal capacity [34]. Treatment with L80 also impaired mammosphere-forming ability, as evidenced by a marked decrease in the number and volume of mammospheres derived from MDA-MB-231 and 4T1 cells ($p < 0.001$, Fig. 4C). Consistent with the *in vitro* data, exposure to L80 significantly reduced the number and volume of mammospheres derived from 4T1 allograft tumors *in vivo* ($p < 0.001$, Fig. 4D). A recent study has shown that HSP90 directly interacts with Oct4 and Nanog and prevents them

from degrading via the ubiquitin proteasome pathway, suggesting that they are potential novel HSP90 client proteins [35]. We observed that L80 significantly downregulates Nanog and Oct4 protein content ($p < 0.01$, Supplementary Fig. S2) in MDA-MB-231 and 4T1 cells, suggesting that downregulation of these pluripotent transcription factors by L80 could contribute to the suppression of breast cancer stem cell-like properties such as mammosphere-forming ability.

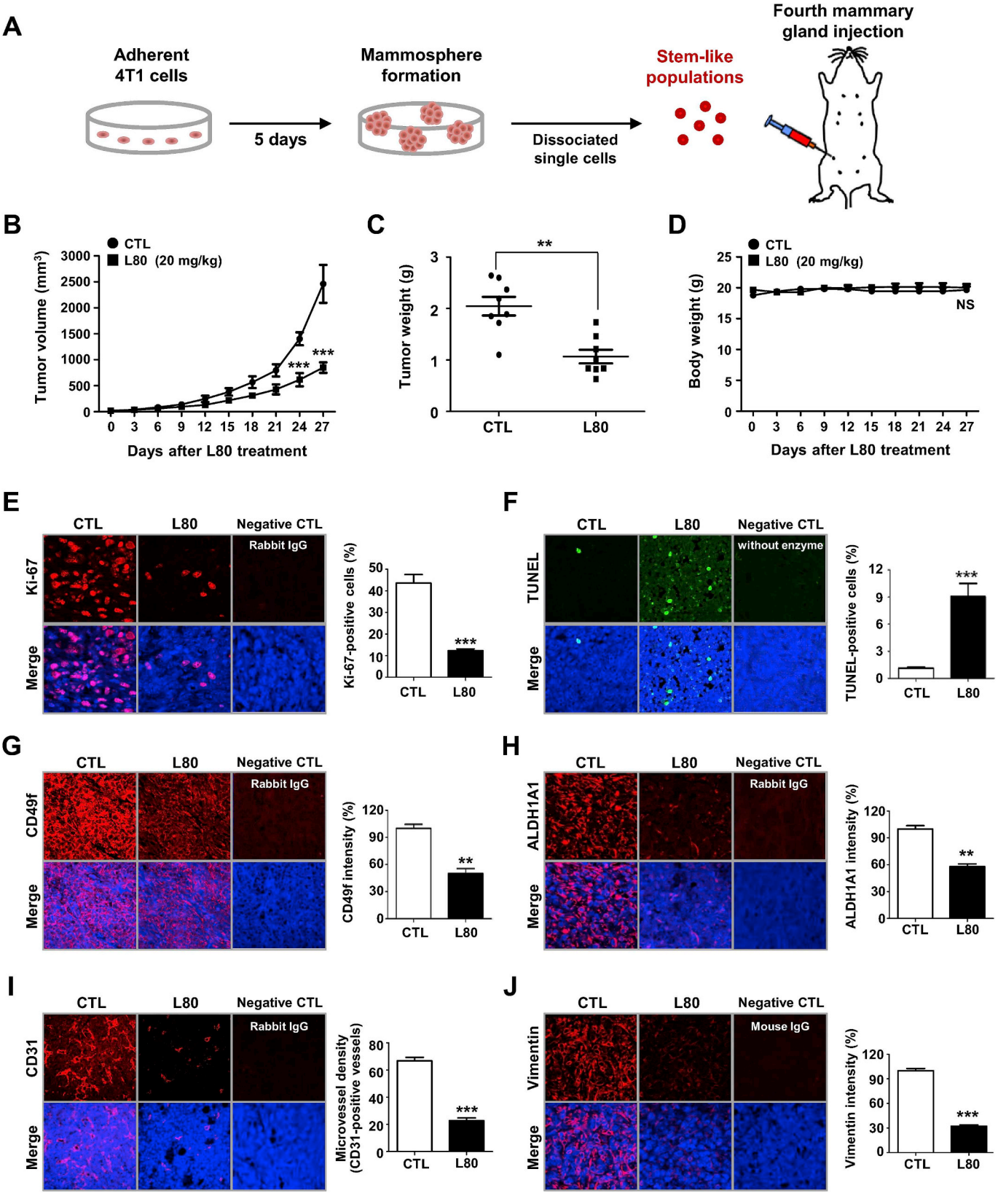

(caption on next page)

Fig. 5. L80 impairs BCSC-enriched TNBC tumors. (A) 8×10^4 cells from mammosphere cultures were orthotopically injected into the duct of the fourth mammary gland of BALB/c female mice. Mice were administered intraperitoneally with L80 (20 mg/kg, every other day) or control solvent for 27 days (n = 8/each group). (B–D) After exposure to L80 or control solvent in allograft mice, tumor growth (B, ***$p < 0.001$), tumor weight (C, **$p < 0.01$) and body weight (D, NS, not significant) were evaluated. (E) Effect of L80 on nuclear Ki-67 expression. Tissue sections were immunostained for Ki-67 (red) or normal rabbit IgG (as a negative control) with DAPI (blue); images are shown at magnification (× 500). The graph represents the percentage of Ki-67-positive cells (bottom panel, ***$p < 0.001$). (F) L80 induces apoptosis *in vivo*, as determined by TUNEL assay. TUNEL buffer without terminal deoxynucleotidyl transferase was used as a negative CTL. The extent of apoptosis is expressed as the percentage of total cells that were TUNEL-positive. More than 1000 cells were analyzed per tumor from each mouse (bottom panel, ***$p < 0.001$). (G–H) Impact of L80 on expression of BCSC markers *in vivo*. Quantitation of fluorescence intensity of CD49f (G, **$p < 0.01$) and ALDH1A1 (H, **$p < 0.01$) signal is shown in the bottom panel, respectively. (I) Inhibition of tumor angiogenesis by L80 administration was determined by microvessel density assay. Tumor tissues were immunostained with CD31 (red) with DAPI, quantitative graphs represent the number of CD31-positive microvessels in intratumoral areas (***$p < 0.001$). (J) L80 administration resulted in a significant downregulation of vimentin expression. A quantitative graph of the vimentin signal intensity is shown in the right panel (***$p < 0.001$). The fluorescence intensities were analyzed using a histogram tool in the Carl Zeiss software package. Normal rabbit IgG or normal mouse IgG was used as negative controls. Data was analyzed by unpaired Student's t-test. (For interpretation of the references to color in this figure legend, the reader is referred to the Web version of this article.)

3.5. L80 attenuates tumor growth via the suppression of BCSC-like properties

4T1 mammospheres were orthotopically injected into the duct of the fourth mammary gland of BALB/c female mice (Fig. 5A). L80 (20 mg/kg, every other day) or control solvent was administrated when the tumor volume reached approximately 50 mm^3. Over the course of 27 days, 4T1 mammosphere-derived tumors subjected to L80 administration exhibited a significant reduction in tumor growth ($p < 0.001$, Fig. 5B) and tumor burden ($p < 0.01$, Fig. 5C), when compared to their control groups. There was no significant change in mean body weight following L80 administration (NS; not significant, Fig. 5D). To confirm the inhibitory effect of L80 on tumor growth, Ki-67 proliferative index was undertaken using allograft tumor tissues. Immunofluorescence staining revealed that the animals receiving L80 exhibited a significant reduction in the number of Ki-67-positive cells ($p < 0.001$, Fig. 5E). Furthermore, the apoptotic index as determined by TUNEL assay revealed that a significant increase in the number of TUNEL-positive cells was observed in the L80-treated animal groups ($p < 0.001$, Fig. 5F).

Our earlier *in vitro* observations demonstrated that L80 effectively targets BCSC-like traits (as shown in Fig. 4). To further investigate this effect, immunostaining analysis for mammary stem cell marker integrin alpha6 (CD49f) and ALDH1A1 was assessed in allograft tumors. Animals receiving L80 exhibited a considerably lower level of CD49f ($p < 0.01$, Fig. 5G) and ALDH1A1 ($p < 0.01$, Fig. 5H) compared to their control counterparts. Since tumor progression is considered to arise in part by stimulation of tumor angiogenesis [36], whether the inhibitory effect of L80 on tumor growth was associated with suppression of angiogenesis was assessed a microvessel density (MVD) assay using the endothelial specific marker cluster of differentiation 31 (CD31). The number of CD31-positive microvessels in the intratumoral area was significantly reduced in the L80-treated groups ($p < 0.001$, Fig. 5I). The major epithelial-mesenchymal transition (EMT) factor vimentin is a well-known substrate of HSP90 and is responsible for cancer cell migration and invasion [37,38]. L80 administration caused a considerable downregulation of vimentin expression ($p < 0.001$, Fig. 5J), which may give rise to the inhibition of cell dissemination.

3.6. L80 suppresses metastasis from primary tumors via dysregulation of STAT3 signaling

We previously reported that BCSC-like characteristics are correlated with higher STAT3 activation and ALDH1 activity as well as enhancement of metastatic potential in TNBC *in vivo* [28]. After L80 administration, BCSC-enriched tumors exhibited a significant reduction in phospho-JAK2 ($p < 0.001$, Fig. 6A) and phospho-STAT3 (Tyr705) expression ($p < 0.01$, Fig. 6B). We next evaluated the impact of L80 on metastasis in allografts derived from 4T1 mammospheres *in vivo*. BLI analysis revealed that mice receiving L80 exhibited a significant reduction in bioluminescence intensity ($p < 0.001$, Fig. 6C). Representative H&E staining further supported the evidence that L80 administration reduced lung and liver metastases ($p < 0.01$, Fig. 6D). The metastatic markers MMP-2 and MMP-9 are STAT3 downstream target genes and their presence promotes metastasis and angiogenesis via the degradation of extracellular matrix components [39–41]. Metastatic control mice exhibited significantly increased MMP-2 and MMP-9 serum levels when compared to normal BALB/c mice of the same age ($p < 0.001$) and these responses were markedly reduced by L80 administration ($p < 0.01$, Fig. 6E and F). Taken together, these findings suggest that L80 results in disruptions of STAT3 activity coinciding with reduced MMP-2 and MMP-9 levels in serum, which may mitigate tumor angiogenesis and metastasis.

4. Discussion

In recent years, there has been renewed interest in the clinical development of HSP90 inhibitors. Although N-terminal HSP90 inhibitors elicit strong anticancer potency in preclinical models, clinical trial outcomes have been unsuccessful due to water solubility issues, low chemical stability, toxicity, and induction of the heat shock response [11,13,22,42,43]. New strategies are needed for targeting HSP90 that provide an appropriate therapeutic balance.

We previously synthesized L80, a deguelin-derivative and a novel C-terminal HSP90 inhibitor. Evidence suggests that L80 elicits anti-proliferative, anti-angiogenic and anti-tumor activity in paclitaxel-resistant non-small cell lung cancer (NSCLC), while exhibiting minimal toxicity toward normal cell lines [25]. It is notable that deguelin treatment resulted in a large number of apoptotic normal cells, while its derivative L80 was more strongly cytotoxic in TNBC cells and less toxic towards normal cells.

The majority of TNBC cases are classified histologically as high-grade invasive ductal carcinomas with aggressive behavior [44,45]. Various chemotherapeutic approaches and combination therapies focus on the suppression of TNBC, and several potential compounds are in clinical trials, including inhibitors of PI3K/AKT, MEK/ERK, and the JAK/STAT3 signaling pathway and an irreversible inhibitor of EGFR [1,4,46,47]. In this context, several potential therapeutic targets for TNBC are also HSP90 client proteins. Our findings show that L80 considerably downregulates AKT, JAK2/STAT3 and MEK/ERK expression.

The role of the STAT3 signaling pathway has been well established in diverse biological functions as well as tumor development, influencing cell survival, motility, invasion, angiogenesis and epithelial to mesenchymal transition [48–50]. STAT3 transcriptional activity is primarily regulated by phosphorylation of the Tyr705 residue which is mediated by JAKs associated with cytokine stimulated receptors and MAPK/ERK [51,52]. Our findings indicate that the STAT3 signaling pathway is interrupted by L80 challenge, as demonstrated by a significant downregulation in phosphorylation of STAT3 and subsequent reduced expression of its downstream target genes cyclin D1 and survivin.

L80 administration also induced a significant reduction in BCSC-like

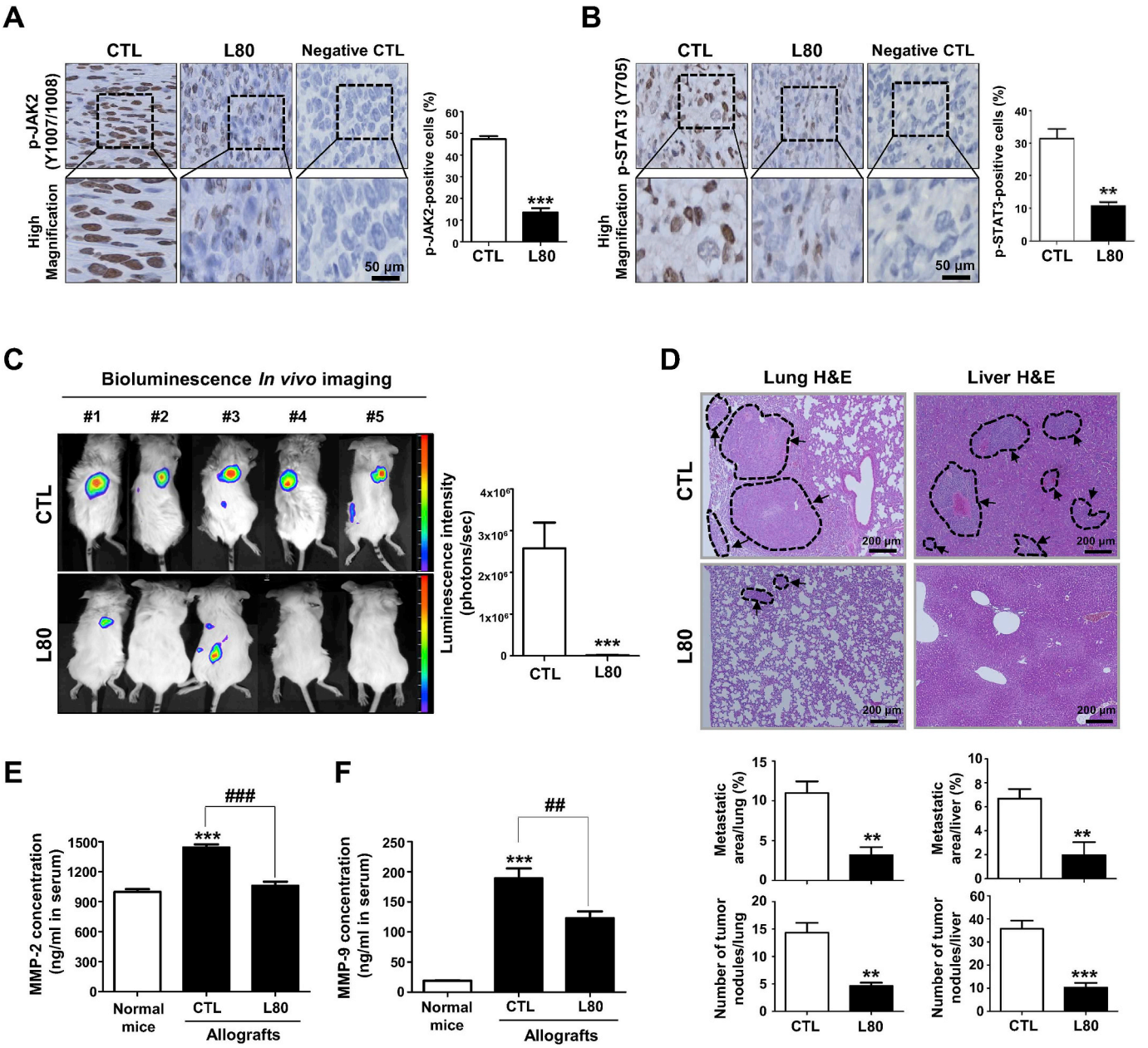

Fig. 6. L80 suppresses distant metastases via JAK2/STAT3 dysregulation *in vivo*. (A–B) Impact of L80 on nuclear expression of phospho-JAK2 and phospho-STAT3 in allografts derived from 4T1 mammospheres. Normal rabbit IgG was used as a negative control. Quantitative graphs of the number of phospho-JAK2-positive cells (A, $***p < 0.001$) and STAT3-positive cells (B, $**p < 0.01$) are shown in the right panel, respectively. (C) Representative bioluminescence imaging (BLI) of metastases is shown for control- and L80-treated groups. D-luciferin sodium salt at 150 mg/kg was administered in mice and subjected to the (BLI) system after removal of the primary tumors. L80-treated syngeneic mice exhibited a dramatic decrease in bioluminescence signal intensity, indicating distant metastases. (D) H&E staining images of lung and liver sections from control and L80-treated mice. The black dotted areas indicate metastatic lesions in the lungs and liver. The number of tumor nodules in lungs ($**p < 0.01$) and liver ($**p < 0.01$) was quantified. (E–F) Effect of L80 on MMP-2 and MMP-9 serum concentrations *in vivo*. Serum was extracted from the CTL- and L80-treated mice and MMP-2 (E) and MMP-9 (F) expression was determined by ELISA assay. Serum from normal mice was used as a negative control. Data were analyzed by Student' t-test ($***p < 0.001$, normal mouse vs control allografts; $##p < 0.01$, control allografts vs L80-treated allografts).

properties, together with the inhibition of ALDH1 activity, suppression of the $CD44^{high}/CD24^{low}$ subpopulation, and the impairment of mammosphere formation *in vitro*. Accumulating evidence indicates that STAT3 is indispensable for the maintenance and self-renewal of CSCs, as it regulates the expression of stem- and differentiation-related genes, while its inhibition resulted in a loss of CSC-like traits, leading to suppression of tumor development and metastasis [28,33,53–56]. Our previous findings also demonstrate that phosphorylated-STAT3 is predominantly elevated in BCSC-like populations such as ALDH + cells and mammospheres derived from TNBC cells [28,32]. Furthermore, BCSC-enriched allografts exhibit enhanced and constitutive STAT3 activation, upregulated CD49f and ALDH1 expression, and more aggressively metastasize to other organs [28]. Consistent with the *in vitro* findings, L80 administration inhibited BCSC-enriched tumor burden, angiogenesis and distal metastatic growth in the lungs and liver via downregulation of BCSC markers. This was interpreted to indicate that L80-induced inhibitory effects on tumor growth may be attributable to the suppression of STAT3 signaling.

MMP-2 and MMP-9 are important determinants of angiogenesis, invasion and cancer metastasis in breast cancer and regulate the degradation and remodeling of basement membranes and the ECM [57–59]. It is noteworthy that the mouse serum ELISA analysis

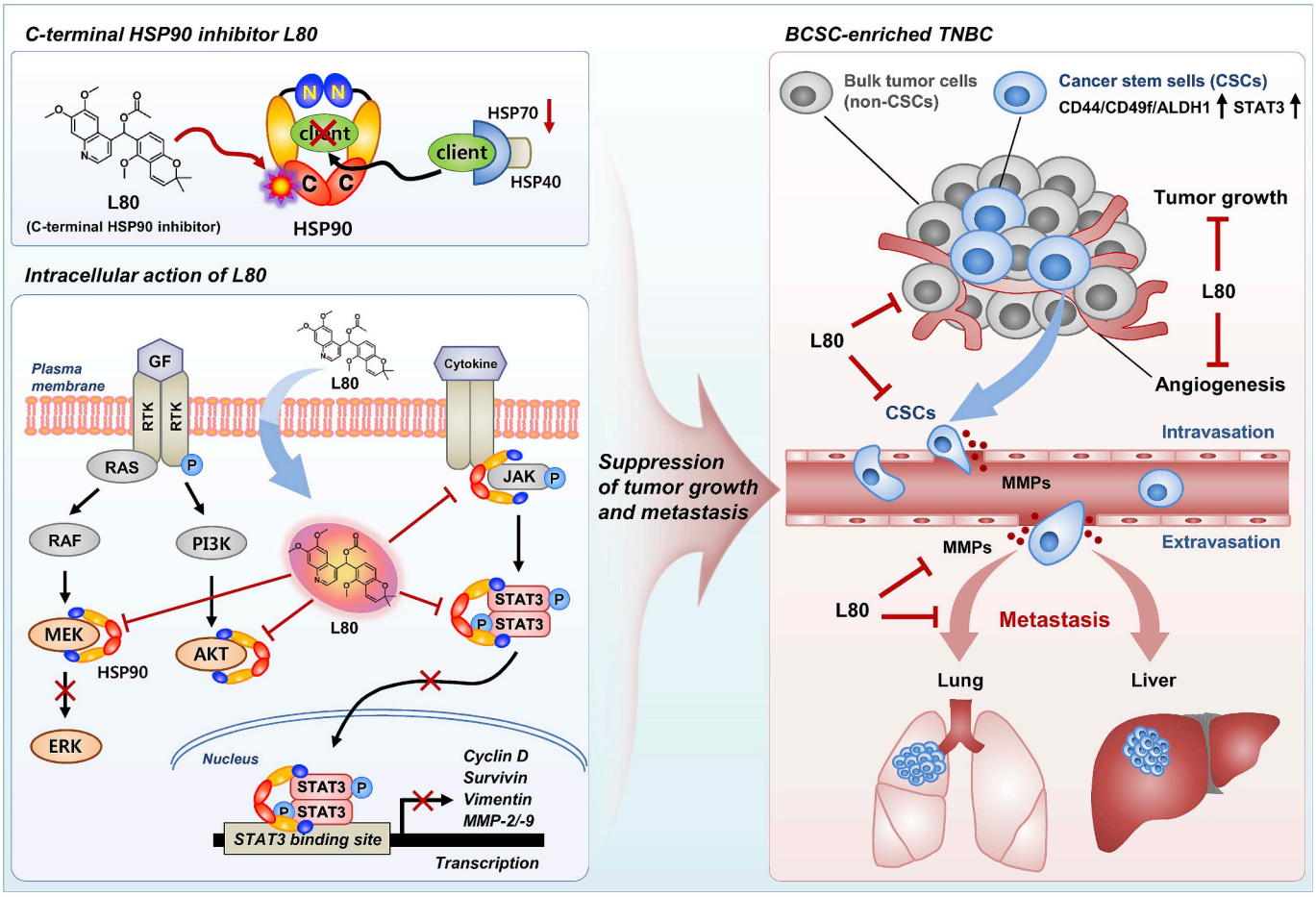

Fig. 7. Hypothetical model illustrating the multiple actions of L80 on tumor growth, angiogenesis and metastasis in triple-negative breast cancer cells. HSP90 directly binds to STAT3, inhibiting STAT3 phosphorylation, dimerization and nuclear translocation, thereby affecting tumor cell survival, proliferation and cancer progression. We propose that (i) L80 inhibits TNBC cell proliferation by suppressing several signaling pathways including AKT, MEK/ERK, and JAK2/STAT3, (ii) L80-induced suppression of BCSC-like traits characterized by reduction of CD44, CD49f, ALDH1 activity and mammosphere-forming ability, (iii) L80 impedes tumor growth, angiogenesis and subsequently suppresses lung and liver metastatic growth, (iv) These phenomena are associated with dysregulation of STAT3 activation, coinciding with downregulation of the downstream factors cyclin D1, survivin, vimentin, and MMP-2/-9.

indicated that MMP-2 and MMP-9 levels in circulating blood were markedly elevated in allografts during metastatic progression and were significantly hampered in the presence of L80 treatment. Accumulating evidence has shown that extracellular HSP90 directly interacts with MMP-2 and MMP-9 to foster their proteolytic activity outside tumor cells, thereby promoting tumor invasiveness and angiogenesis. These responses can be attenuated by HSP90 inhibition or a HSP90 monoclonal antibody [60–62]. It is conceivable that L80 at least in part inhibits extracellular HSP90 leading to a reduction in MMP levels, which likely contributes to the impairment of tumor angiogenesis and metastatic spread.

In summary, we have demonstrated that the C-terminal HSP90 inhibitor L80 inhibits TNBC cell proliferation via the suppression of several signaling pathways including AKT, MEK/ERK and JAK2/STAT3 as well as BCSC-like traits such as CD44, CD49f and ALDH1 activity. L80 administration impaired tumor growth, angiogenesis, and distant metastasis via dysregulation of STAT3 activation (Fig. 7). These findings suggest that L80 may offer an effective therapeutic pathway for the simultaneous targeting of both HSP90 and STAT3 for the treatment of TNBC.

Conflicts of interest

The authors declare no conflict of interest.

Author contributions

Conception and design: JY. Kim, J. Lee and JH. Seo.

Performed the experiments: T-M. Cho, JY. Kim, E. Oh, Y-J. Kim, D. Sung and S. Jung.

Analyzed the data: T-M. Cho, Y-J. Kim, L. Farrand and JY. Kim.

Contributed reagents, materials and analysis tools: T-M. Cho, JY. Kim, E. Oh, Y-J. Kim and JH. Seo.

Synthesis of L80: V-H. Hoang, C-T. Nguyen and J. Ann.

Wrote the paper: JY. Kim, L. Farrand and T-M. Cho.

Final approval manuscript: T-M. Cho, Y-J. Kim, E. Oh, D. Sung, L. Farrand, V-H. Hoang, C-T. Nguyen, J. Ann, S. Jung, JH. Seo and J. Lee.

Acknowledgments

This research was supported by a grant from the Korea Health Technology R&D Project through the Korea Health Industry Development Institute (KHIDI), funded by the Ministry of Health & Welfare, Republic of Korea (grant number: HI12C1852, HA17C0053), a National Research Foundation of Korea (NRF) grant, funded by the Ministry of Science, ICT & Future Planning (MSIP, grant number: 2018R1A2B6005347, 2018R1D1A1B07045416, 2015R1C1A2A01053747, 2017R1A6A3A11029467) and the Brain Korea (BK) 21 Plus Program.

Appendix A. Supplementary data

Supplementary data to this article can be found online at https://doi.org/10.1016/j.canlet.2019.01.029.

References

[1] M. Kalimutho, K. Parsons, D. Mittal, J.A. Lopez, S. Srihari, K.K. Khanna, Targeted therapies for triple-negative breast cancer: combating a stubborn disease, Trends Pharmacol. Sci. 36 (2015) 822–846.

[2] N.A. Soliman, S.M. Yussif, Ki-67 as a prognostic marker according to breast cancer molecular subtype, Canc. Biol. Med. 13 (2016) 496–504.

[3] H. Li, X. Han, Y. Liu, G. Liu, G. Dong, Ki67 as a predictor of poor prognosis in patients with triple-negative breast cancer, Oncol. Lett. 9 (2015) 149–152.

[4] R. Dent, M. Trudeau, K.I. Pritchard, W.M. Hanna, H.K. Kahn, C.A. Sawka, L.A. Lickley, E. Rawlinson, P. Sun, S.A. Narod, Triple-negative breast cancer: clinical features and patterns of recurrence, Clin. Canc. Res. 13 (2007) 4429–4434.

[5] W.B. Pratt, D.O. Toft, Regulation of signaling protein function and trafficking by the hsp90/hsp70-based chaperone machinery, Exp. Biol. Med. (Maywood) 228 (2003) 111–133.

[6] M. Ferrarini, S. Heltai, M.R. Zocchi, C. Rugarli, Unusual expression and localization of heat-shock proteins in human tumor cells, Int. J. Canc. 51 (1992) 613–619.

[7] J.S. Isaacs, W. Xu, L. Neckers, Heat shock protein 90 as a molecular target for cancer therapeutics, Cancer Cell 3 (2003) 213–217.

[8] L. Neckers, Heat shock protein 90: the cancer chaperone, J. Biosci. 32 (2007) 517–530.

[9] F.H. Schopf, M.M. Biebl, J. Buchner, The HSP90 chaperone machinery, Nat. Rev. Mol. Cell Biol. 18 (2017) 345–360.

[10] Q. Cheng, J.T. Chang, J. Geradts, L.M. Neckers, T. Haystead, N.L. Spector, H.K. Lyerly, Amplification and high-level expression of heat shock protein 90 marks aggressive phenotypes of human epidermal growth factor receptor 2 negative breast cancer, Breast Cancer Res. 14 (2012) R62.

[11] L. Neckers, P. Workman, Hsp90 molecular chaperone inhibitors: are we there yet? Clin. Canc. Res. 18 (2012) 64–76.

[12] J.E. Bohonowych, U. Gopal, J.S. Isaacs, Hsp90 as a gatekeeper of tumor angiogenesis: clinical promise and potential pitfalls, J. Oncol. 2010 (2010) 412985.

[13] S. Modi, A. Stopeck, H. Linden, D. Solit, S. Chandarlapaty, N. Rosen, G. D'Andrea, M. Dickler, M.E. Moynahan, S. Sugarman, W. Ma, S. Patil, L. Norton, A.L. Hannah, C. Hudis, HSP90 inhibition is effective in breast cancer: a phase II trial of tanespimycin (17-AAG) plus trastuzumab in patients with HER2-positive metastatic breast cancer progressing on trastuzumab, Clin. Canc. Res. 17 (2011) 5132–5139.

[14] S. Tsutsumi, K. Beebe, L. Neckers, Impact of heat-shock protein 90 on cancer metastasis, Future Oncol. 5 (2009) 679–688.

[15] C.E. Bocchini, M.M. Kasembeli, S.H. Roh, D.J. Tweardy, Contribution of chaperones to STAT pathway signaling, JAK-STAT 3 (2014) e970459.

[16] M.P. Moreira, L. da Conceicao Braga, G.D. Cassali, L.M. Silva, STAT3 as a promising chemoresistance biomarker associated with the CD44(+/high)/CD24(-/low)/ALDH(+) BCSCs-like subset of the triple-negative breast cancer (TNBC) cell line, Exp. Cell Res. 363 (2018) 283–290.

[17] S.R. Sirkisoon, R.L. Carpenter, T. Rimkus, A. Anderson, A. Harrison, A.M. Lange, G. Jin, K. Watabe, H.W. Lo, Interaction between STAT3 and GLI1/tGLI1 oncogenic transcription factors promotes the aggressiveness of triple-negative breast cancers and HER2-enriched breast cancer, Oncogene 37 (2018) 2502–2514.

[18] S.J. Thomas, J.A. Snowden, M.P. Zeidler, S.J. Danson, The role of JAK/STAT signalling in the pathogenesis, prognosis and treatment of solid tumours, Br. J. Canc. 113 (2015) 365–371.

[19] H. Xin, A. Herrmann, K. Reckamp, W. Zhang, S. Pal, M. Hedvat, C. Zhang, W. Liang, A. Scuto, S. Weng, D. Morosini, Z.A. Cao, M. Zinda, R. Figlin, D. Huszar, R. Jove, H. Yu, Antiangiogenic and antimetastatic activity of JAK inhibitor AZD1480, Cancer Res. 71 (2011) 6601–6610.

[20] K. Banerjee, H. Resat, Constitutive activation of STAT3 in breast cancer cells: a review, Int. J. Canc. 138 (2016) 2570–2578.

[21] M. Chatterjee, S. Jain, T. Stuhmer, M. Andrulis, U. Ungethum, R.J. Kuban, H. Lorentz, K. Bommert, M. Topp, D. Kramer, H.K. Muller-Hermelink, H. Einsele, A. Greiner, R.C. Bargou, STAT3 and MAPK signaling maintain overexpression of heat shock proteins 90alpha and beta in multiple myeloma cells, which critically contribute to tumor-cell survival, Blood 109 (2007) 720–728.

[22] R. Garcia-Carbonero, A. Carnero, L. Paz-Ares, Inhibition of HSP90 molecular chaperones: moving into the clinic, Lancet Oncol. 14 (2013) e358–369.

[23] X. Wang, M. Chen, J. Zhou, X. Zhang, HSP27, 70 and 90, anti-apoptotic proteins, in clinical cancer therapy (Review), Int. J. Oncol. 45 (2014) 18–30.

[24] M.V. Powers, P.A. Clarke, P. Workman, Death by chaperone: HSP90, HSP70 or both? Cell Cycle 8 (2009) 518–526.

[25] S.C. Lee, H.Y. Min, H. Choi, H.S. Kim, K.C. Kim, S.J. Park, M.A. Seong, J.H. Seo, H.J. Park, Y.G. Suh, K.W. Kim, H.S. Hong, H. Kim, M.Y. Lee, J. Lee, H.Y. Lee, Synthesis and evaluation of a novel deguelin derivative, L80, which disrupts ATP binding to the C-terminal domain of heat shock protein 90, Mol. Pharmacol. 88 (2015) 245–255.

[26] E. Oh, J.Y. Kim, Y. Cho, H. An, N. Lee, H. Jo, C. Ban, J.H. Seo, Overexpression of angiotensin II type 1 receptor in breast cancer cells induces epithelial-mesenchymal transition and promotes tumor growth and angiogenesis, Biochim. Biophys. Acta 1863 (2016) 1071–1081.

[27] Y.J. Kim, D. Sung, E. Oh, Y. Cho, T.M. Cho, L. Farrand, J.H. Seo, J.Y. Kim, Flubendazole overcomes trastuzumab resistance by targeting cancer stem-like properties and HER2 signaling in HER2-positive breast cancer, Cancer Lett. 412 (2018) 118–130.

[28] E. Oh, Y.J. Kim, H. An, D. Sung, T.M. Cho, L. Farrand, S. Jang, J.H. Seo, J.Y. Kim, Flubendazole elicits anti-metastatic effects in triple-negative breast cancer via STAT3 inhibition, Int. J. Canc. 143 (2018) 1978–1993.

[29] J.Y. Kim, Y. Cho, E. Oh, N. Lee, H. An, D. Sung, T.M. Cho, J.H. Seo, Disulfiram targets cancer stem-like properties and the HER2/Akt signaling pathway in HER2-positive breast cancer, Cancer Lett. 379 (2016) 39–48.

[30] L.L. Marotta, V. Almendro, A. Marusyk, M. Shipitsin, J. Schemme, S.R. Walker, N. Bloushtain-Qimron, J.J. Kim, S.A. Choudhury, R. Maruyama, Z. Wu, M. Gonen, L.A. Mulvey, M.O. Bessarabova, S.J. Huh, S.J. Silver, S.Y. Kim, S.Y. Park, H.E. Lee, K.S. Anderson, A.L. Richardson, T. Nikolskaya, Y. Nikolsky, X.S. Liu, D.E. Root, W.C. Hahn, D.A. Frank, K. Polyak, The JAK2/STAT3 signaling pathway is required for growth of CD44(+)CD24(-) stem cell-like breast cancer cells in human tumors, J. Clin. Invest. 121 (2011) 2723–2735.

[31] E. Prinsloo, A.H. Kramer, A.L. Edkins, G.L. Blatch, STAT3 interacts directly with Hsp90, IUBMB Life 64 (2012) 266–273.

[32] Y.J. Kim, J.Y. Kim, N. Lee, E. Oh, D. Sung, T.M. Cho, J.H. Seo, Disulfiram suppresses cancer stem-like properties and STAT3 signaling in triple-negative breast cancer cells, Biochem. Biophys. Res. Commun. 486 (2017) 1069–1076.

[33] W. Wei, D.J. Tweardy, M. Zhang, X. Zhang, J. Landua, I. Petrovic, W. Bu, K. Roarty, S.G. Hilsenbeck, J.M. Rosen, M.T. Lewis, STAT3 signaling is activated preferentially in tumor-initiating cells in claudin-low models of human breast cancer, Stem Cell. 32 (2014) 2571–2582.

[34] G. Dontu, W.M. Abdallah, J.M. Foley, K.W. Jackson, M.F. Clarke, M.J. Kawamura, M.S. Wicha, In vitro propagation and transcriptional profiling of human mammary stem/progenitor cells, Genes Dev. 17 (2003) 1253–1270.

[35] E. Bradley, E. Bieberich, N.F. Mivechi, D. Tangpisuthipongsa, G. Wang, Regulation of embryonic stem cell pluripotency by heat shock protein 90, Stem Cell. 30 (2012) 1624–1633.

[36] N. Nishida, H. Yano, T. Nishida, T. Kamura, M. Kojiro, Angiogenesis in cancer, Vasc. Health Risk Manag. 2 (2006) 213–219.

[37] M.H. Zhang, J.S. Lee, H.J. Kim, D.I. Jin, J.I. Kim, K.J. Lee, J.S. Seo, HSP90 protects apoptotic cleavage of vimentin in geldanamycin-induced apoptosis, Mol. Cell. Biochem. 281 (2006) 111–121.

[38] M.G. Mendez, S. Kojima, R.D. Goldman, Vimentin induces changes in cell shape, motility, and adhesion during the epithelial to mesenchymal transition, FASEB J. 24 (2010) 1838–1851.

[39] R.L. Carpenter, H.W. Lo, STAT3 target genes relevant to human cancers, Cancers (Basel) 6 (2014) 897–925.

[40] S.L. Raza, L.A. Cornelius, Matrix metalloproteinases: pro- and anti-angiogenic activities, J. Invest. Dermatol. Symp. Proc. 5 (2000) 47–54.

[41] L.E. Littlepage, M.D. Sternlicht, N. Rougier, J. Phillips, E. Gallo, Y. Yu, K. Williams, A. Brenot, J.I. Gordon, Z. Werb, Matrix metalloproteinases contribute distinct roles in neuroendocrine prostate carcinogenesis, metastasis, and angiogenesis progression, Cancer Res. 70 (2010) 2224–2234.

[42] K. Sidera, E. Patsavoudi, HSP90 inhibitors: current development and potential in cancer therapy, Recent Pat. Anti-Cancer Drug Discov. 9 (2014) 1–20.

[43] M.A. Biamonte, R. Van de Water, J.W. Arndt, R.H. Scannevin, D. Perret, W.C. Lee, Heat shock protein 90: inhibitors in clinical trials, J. Med. Chem. 53 (2010) 3–17.

[44] R. Schmadeka, B.E. Harmon, M. Singh, Triple-negative breast carcinoma: current and emerging concepts, Am. J. Clin. Pathol. 141 (2014) 462–477.

[45] E. Montagna, P. Maisonneuve, N. Rotmensz, G. Cancello, M. Iorfida, A. Balduzzi, V. Galimberti, P. Veronesi, A. Luini, G. Pruneri, L. Bottiglieri, M.G. Mastropasqua, A. Goldhirsch, G. Viale, M. Colleoni, Heterogeneity of triple-negative breast cancer: histologic subtyping to inform the outcome, Clin. Breast Canc. 13 (2013) 31–39.

[46] J.R. Jhan, E.R. Andrechek, Triple-negative breast cancer and the potential for targeted therapy, Pharmacogenomics 18 (2017) 1595–1609.

[47] C.A. Hudis, L. Gianni, Triple-negative breast cancer: an unmet medical need, Oncologist 16 (Suppl 1) (2011) 1–11.

[48] M.K. Wendt, N. Balanis, C.R. Carlin, W.P. Schiemann, STAT3 and epithelial-mesenchymal transitions in carcinomas, JAK-STAT 3 (2014) e28975.

[49] D. Wei, X. Le, L. Zheng, L. Wang, J.A. Frey, A.C. Gao, Z. Peng, S. Huang, H.Q. Xiong, J.L. Abbruzzese, K. Xie, Stat3 activation regulates the expression of vascular endothelial growth factor and human pancreatic cancer angiogenesis and metastasis, Oncogene 22 (2003) 319–329.

[50] M.Z. Kamran, P. Patil, R.P. Gude, Role of STAT3 in cancer metastasis and translational advances, BioMed Res. Int. 2013 (2013) 421821.

[51] C.P. Lim, X. Cao, Regulation of Stat3 activation by MEK kinase 1, J. Biol. Chem. 276 (2001) 21004–21011.

[52] Y.P. Liu, Y.N. Tan, Z.L. Wang, L. Zeng, Z.X. Lu, L.L. Li, W. Luo, M. Tang, Y. Cao, Phosphorylation and nuclear translocation of STAT3 regulated by the Epstein-Barr virus latent membrane protein 1 in nasopharyngeal carcinoma, Int. J. Mol. Med. 21 (2008) 153–162.

[53] L. Lin, B. Hutzen, H.F. Lee, Z. Peng, W. Wang, C. Zhao, H.J. Lin, D. Sun, P.K. Li, C. Li, H. Korkaya, M.S. Wicha, J. Lin, Evaluation of STAT3 signaling in ALDH+ and ALDH+/CD44+/CD24- subpopulations of breast cancer cells, PLoS One 8 (2013) e82821.

[54] M.M. Sherry, A. Reeves, J.K. Wu, B.H. Cochran, STAT3 is required for proliferation and maintenance of multipotency in glioblastoma stem cells, Stem Cell. 27 (2009) 2383–2392.

[55] R. Thakur, R. Trivedi, N. Rastogi, M. Singh, D.P. Mishra, Inhibition of STAT3, FAK and Src mediated signaling reduces cancer stem cell load, tumorigenic potential and metastasis in breast cancer, Sci. Rep. 5 (2015) 10194.

[56] H. Zhang, K. Cai, J. Wang, X. Wang, K. Cheng, F. Shi, L. Jiang, Y. Zhang, J. Dou, MiR-7, inhibited indirectly by lincRNA HOTAIR, directly inhibits SETDB1 and

reverses the EMT of breast cancer stem cells by downregulating the STAT3 pathway, Stem Cell. 32 (2014) 2858–2868.
[57] A. Merdad, S. Karim, H.J. Schulten, A. Dallol, A. Buhmeida, F. Al-Thubaity, M.A. Gari, A.G. Chaudhary, A.M. Abuzenadah, M.H. Al-Qahtani, Expression of matrix metalloproteinases (MMPs) in primary human breast cancer: MMP-9 as a potential biomarker for cancer invasion and metastasis, Anticancer Res. 34 (2014) 1355–1366.
[58] C. Gialeli, A.D. Theocharis, N.K. Karamanos, Roles of matrix metalloproteinases in cancer progression and their pharmacological targeting, FEBS J. 278 (2011) 16–27.
[59] Y. Sullu, G.G. Demirag, A. Yildirim, F. Karagoz, B. Kandemir, Matrix metalloproteinase-2 (MMP-2) and MMP-9 expression in invasive ductal carcinoma of the breast, Pathol. Res. Pract. 207 (2011) 747–753.
[60] X. Song, X. Wang, W. Zhuo, H. Shi, D. Feng, Y. Sun, Y. Liang, Y. Fu, D. Zhou, Y. Luo, The regulatory mechanism of extracellular Hsp90{alpha} on matrix metalloproteinase-2 processing and tumor angiogenesis, J. Biol. Chem. 285 (2010) 40039–40049.
[61] B.K. Eustace, T. Sakurai, J.K. Stewart, D. Yimlamai, C. Unger, C. Zehetmeier, B. Lain, C. Torella, S.W. Henning, G. Beste, B.T. Scroggins, L. Neckers, L.L. Ilag, D.G. Jay, Functional proteomic screens reveal an essential extracellular role for hsp90 alpha in cancer cell invasiveness, Nat. Cell Biol. 6 (2004) 507–514.
[62] D. Stellas, A. El Hamidieh, E. Patsavoudi, Monoclonal antibody 4C5 prevents activation of MMP2 and MMP9 by disrupting their interaction with extracellular HSP90 and inhibits formation of metastatic breast cancer cell deposits, BMC Cell Biol. 11 (2010) 51.